

## A Appendix

### A.1 Detailed Derivation of Hierarchical Operational Space Control (H-OSC)

Hierarchical Operational Space Control (H-OSC) ensures the execution of multiple objectives with a strict priority ordering. Consider an  $n$ -DOF robot manipulator described by dynamics:

$$\mathbf{M}(\mathbf{q})\ddot{\mathbf{q}} + \mathbf{C}(\mathbf{q}, \dot{\mathbf{q}}) + \mathbf{g}(\mathbf{q}) = \boldsymbol{\tau},$$

where  $\mathbf{q} \in \mathbb{R}^n$  is the joint configuration,  $\mathbf{M}(\mathbf{q}) \in \mathbb{R}^{n \times n}$  is the inertia matrix,  $\mathbf{C}(\mathbf{q}, \dot{\mathbf{q}}) \in \mathbb{R}^n$  are the Coriolis and centrifugal terms, and  $\mathbf{g}(\mathbf{q}) \in \mathbb{R}^n$  represents gravity torques.

Given a ranked set of objectives  $\sigma_t = \{j_1, j_2, \dots, j_{|\mathcal{J}_t|}\}$ , H-OSC calculates command torques by recursively projecting control inputs into null spaces defined by higher-priority tasks:

$$\boldsymbol{\tau} = \sum_{j \in \mathcal{J}_t} \mathbf{N}_j \boldsymbol{\tau}_j,$$

where the unprojected torque for objective  $j$  is computed as:

$$\boldsymbol{\tau}_j = \bar{\mathbf{J}}_j^T \mathbf{f}_j,$$

and the null-space projection matrix  $\mathbf{N}_j$  is recursively defined by:

$$\mathbf{N}_{j+1} = \mathbf{N}_j - \mathbf{J}_j^\# \bar{\mathbf{J}}_j \mathbf{N}_j, \quad \mathbf{N}_1 = \mathbf{I}.$$

Here,  $\mathbf{J}_j$  is the Jacobian associated with objective  $j$ , and  $\bar{\mathbf{J}}_j = \mathbf{J}_j \mathbf{N}_j$  is the null-space projected Jacobian. The generalized inverse Jacobian  $\mathbf{J}_j^\#$  is given by:

$$\mathbf{J}_j^\# = \mathbf{M}^{-1} \bar{\mathbf{J}}_j^T (\bar{\mathbf{J}}_j \mathbf{M}^{-1} \bar{\mathbf{J}}_j^T)^{-1}.$$

Operational-space dynamics for each task  $j$  can be expressed as:

$$\boldsymbol{\Lambda}_j \ddot{\mathbf{x}}_j + \boldsymbol{\mu}_j + \mathbf{g}_j = \mathbf{f}_j,$$

where:

- $\boldsymbol{\Lambda}_j = \mathbf{J}_j^{-T} \mathbf{M} \mathbf{J}_j^{-1}$  is the operational-space inertia matrix,
- $\boldsymbol{\mu}_j = \mathbf{J}_j^{-T} \mathbf{C} - \boldsymbol{\Lambda}_j \dot{\mathbf{J}}_j \dot{\mathbf{q}}$  captures Coriolis and centrifugal effects,
- $\mathbf{g}_j = \mathbf{J}_j^{-T} \mathbf{g}$  represents gravitational forces in task space.

For each objective, a desired operational-space acceleration  $\ddot{\mathbf{x}}_j$  is chosen based on the task requirements:

**Pose Control Objective:** uses a PD control law:

$$\ddot{\mathbf{x}}_{\text{pose}} = \ddot{\mathbf{x}}_g + \mathbf{K}_p(\mathbf{x}_g - \mathbf{x}) + \mathbf{K}_d(\dot{\mathbf{x}}_g - \dot{\mathbf{x}}).$$

**Force Control Objective:** matches desired contact forces:

$$\ddot{\mathbf{x}}_{\text{force}} = -\mathbf{K}_f(\mathbf{f}_j - \mathbf{f}_j^{\text{des}}).$$

Operational-space forces  $\mathbf{f}_j$  are converted into joint torques:

$$\boldsymbol{\tau}_j = \bar{\mathbf{J}}_j^T \mathbf{f}_j,$$

and projected using null-space matrices to ensure non-interference with higher-priority objectives.

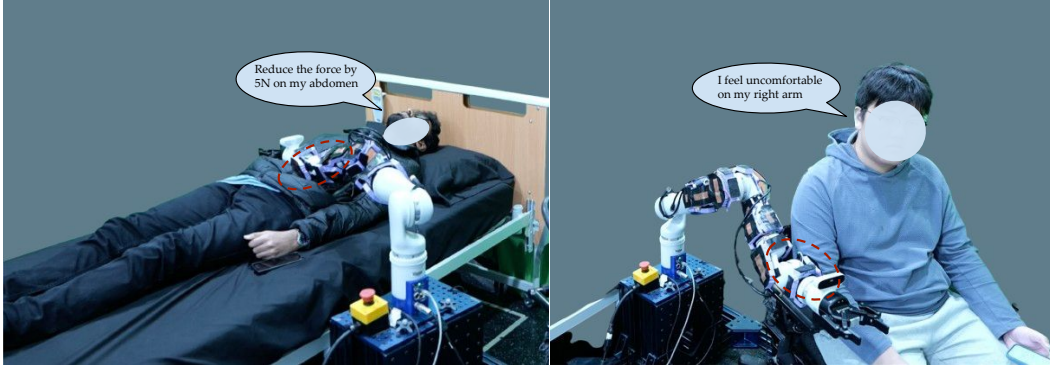


Figure 8: User study setup for comparing different feedback mechanisms in two different configurations. *Left* shows the participant lying down on the bed along with an example of the magnitude-based feedback, and *Right* shows the participant sitting on a wheelchair with an example of the descriptive feedback.

## A.2 Simulating User Feedback

We create a user model by initializing a base priority ID and comfort threshold for each body part. Given contact forces at timestep  $t$ , we compare the forces with the corresponding force thresholds. In case there is a body part for which the forces are above the threshold and the degree by which the forces are off. Using a sensitivity ratio (see Sec. V), which is a function of the comfort threshold itself, we generate the feedback for this body part. In case of multiple violations, we use the base priority ID to decide which body part to generate feedback for. Feedback is generated for body parts with higher base priority unless the force violation is beyond a safety force limit (set manually and the same for each user).

## A.3 Comparison of Feedback Mechanisms Using NASA-TLX

Our system currently solicits user feedback in a *descriptive* form, where users describe the affected body part and how they feel (e.g., “I feel slightly uncomfortable around my abdomen”). An alternative is *magnitude-based* feedback, in which users specify a numerical change in force (in Newtons). While magnitude-based feedback offers more precision, we hypothesize that most users prefer providing descriptive input due to the lower mental burden of recalling numeric force values. To investigate this, we conducted a Wizard-of-Oz study comparing these two feedback mechanisms via a modified NASA-TLX workload assessment.

**Study Procedure.** We recruited 11 participants (8 male, 3 female; ages 21–28) without mobility limitations. Each participant experienced two configurations (see Figure 8): i) sitting in a wheelchair with the robot’s forearm contacting their right arm, and ii) lying on a bed with the robot’s forearm or upper arm contacting their lower abdomen. For each configuration, participants performed a separate trial under each of the two feedback mechanisms. At the end of every trial, they rated the method on a 5-point Likert scale for mental demand, hurriedness, and irritation. We repeated each configuration two times, counterbalancing the order of feedback mechanisms across participants. This study was approved by our organization’s Institutional Review Board, and all participants provided written consent.

**Results and Analysis.** Ten of the 11 participants preferred description-based feedback. Figure 9 shows that description-based feedback yielded significantly lower cognitive workload than the magnitude-based approach. A paired-sample  $t$ -test indicated statistically significant differences in mental demand ( $p < 0.001$ ), hurriedness ( $p < 0.05$ ), and irritation ( $p < 0.001$ ) between the two methods. These findings support our hypothesis that descriptive feedback results in significantly lower mental burden, presenting a reasonable tradeoff between ease of feedback and precision of feedback.

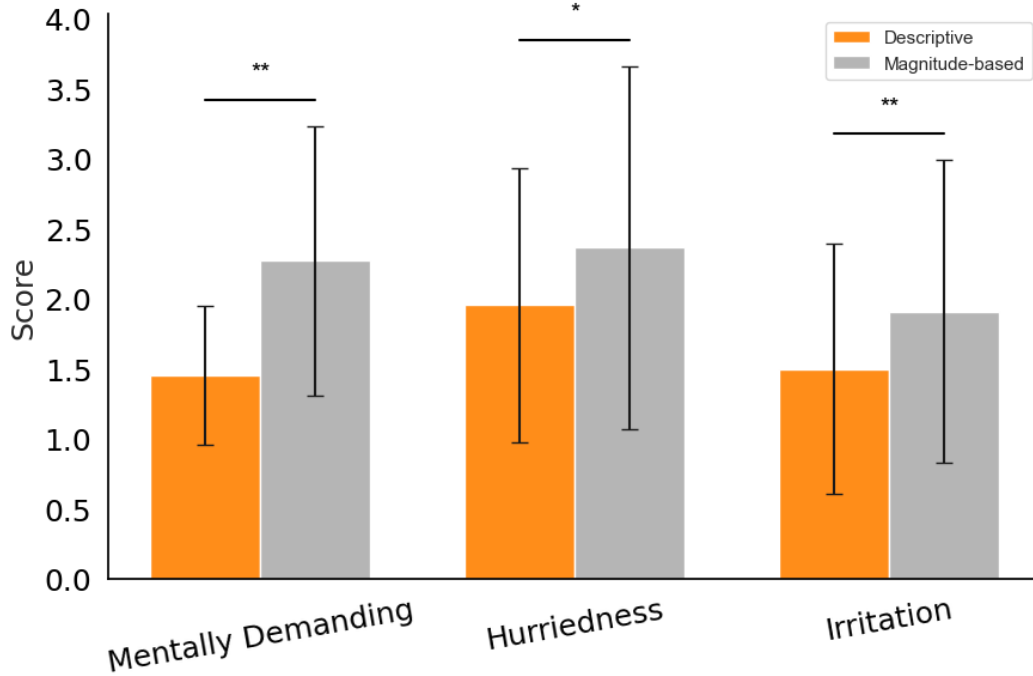


Figure 9: User study with 11 participants. Description-based feedback yields significantly lower cognitive workload (lower score is better) than magnitude-based controls.

#### A.4 Additional System Details

Sensors are modeled as soft bodies in Obi (Unity) and made using piezoresistive taxels in the real-world implementation. Each sensor provides contact location and force data. We integrate these sensor readings with H-OSC implemented using PyBullet [37]. H-OSC with LinUCB-Rank can operate at up to approximately 250 Hz, interfacing with a compliant low-level controller (1 kHz), ensuring robust handling of abrupt motions, such as muscle spasms. After stabilization, the system quickly refocuses on reference trajectories.

#### A.5 Appendix: Additional Details of Contact Preference User Study

**Study Procedure.** Participants were recruited via Tetra Insights, a platform providing financially compensated, high-quality respondents. Our study was approved by our Institutional Review Board. Each participant was asked to envision a home-helper robot with a human-like form factor depicted through a hand-sketched illustration featuring inflated, soft materials. Participants indicated their comfort with robot-initiated touch on a graphical interface that included 37 predefined body regions, identified with input from two medical doctors (general practitioners). Participants also had the option to provide additional insights through open-ended responses.

**Participant Demographics.** The study included 98 adults (ages 32–77, mean age 58), of whom 42 participants were aged 65 or older and 56 were younger. Among participants, 67 identified as female (including 1 transgender female), and 31 identified as male. Forty-nine participants reported having a disability, 42 reported past injuries, and 7 chose not to disclose.

**Detailed Findings.** Overall, 40% of participants provided detailed open-ended responses elaborating on their choices. Arms and hands received the highest number of selections (779 total) across all touch categories. Right-handed participants specifically favored their dominant arm or hand for lighter supportive tasks, whereas the upper and lower back regions were predominantly selected for scenarios involving more substantial support or bracing. Regions such as the buttocks and genitals received minimal selections across all categories, highlighting privacy and comfort boundaries. Fin-

gers and toes were deliberately excluded, as assistive interactions typically involve broader body regions.

## A.6 Real-world user study with human subjects

**Study Procedure.** Participants first received an introduction describing the purpose of the study—evaluating two robotic arm control methods designed for robot-assisted caregiving involving whole-arm contact. Participants were informed about the specific caregiving scenario (bed bathing), their evaluation tasks (performance in clearing artificial dirt (ground coffee), perceived safety, and comfort), and how to provide verbal feedback during uncomfortable contacts. Before experimental trials, participants completed a supervised sample trial to practice providing feedback and simulating a person with mobility limitations. They used a provided digital questionnaire to record evaluations after each trial, identified via method IDs. In the actual trials, each participant experienced two distinct contact configurations across two methods, with two trajectories each (wiping arm and leg). Participants were repeatedly reminded to keep their responses independent of previous trials and to remain stationary during contact interactions. After completing all trials, participants filled out a final questionnaire before concluding the study.

Below are the results from the study conducted with 8 participants with no visible mobility limitations.

Table 1: User-study ratings (mean  $\pm$  SD on a 1–5 Likert scale).

	Task Perf.	Safety	Comfort
Heuristic	$2.53 \pm 0.94$	$4.59 \pm 0.71$	$4.65 \pm 0.61$
LinUCB-Rank (Ours)	$3.06 \pm 0.97$	$4.65 \pm 0.61$	$4.82 \pm 0.39$

In the post-study questionnaire, participants were asked to select which of the two methods they would prefer for caregiving applications involving whole-arm contact. Seven out of eight participants preferred our method.

## A.7 Additional Experiments

### Simulation-in-the-Loop Learning: Pauses and Accuracy.

*Pauses:* We measured execution times for preference learning convergence in simulation ( $52.4 \pm 21.7$ s). These pauses reduced progressively (to  $\sim 30$ s) as user-contact preference estimates improved, indicating suitability for online use.

*Simulation Fidelity (Sim-to-Real Gap):* To test robustness to simulation inaccuracies, we varied the fidelity of the digital twin’s collision model (quality = 1: exact fit to visual mesh; quality = 0.75: 75% fit). Lower fidelity led to only a modest (12.21%) increase in required feedback signals, demonstrating our method’s resilience.

### Comparison with Alternative Baselines.

We evaluated PrioriTouCh against two additional baselines:

- *Residual Reinforcement Learning:* Did not achieve stable convergence within our online-learning constraints, showing no force-violation reduction even after 20 minutes of training.
- *Jain et al.’s MPC-based whole-arm manipulation (IJRR 2013):* Adapted to our trajectories, this baseline resulted in roughly 3x more force-threshold violations than PrioriTouCh.